

PACS numbers: 87.64.Cc; 42.30.Wb, 43.35.Sx
DOI: 10.1070/QE2012v042n05ABEH014889

Acoustooptical visualisation of biological media using multislit diaphragms

A.P. Solov'ev, M.I. Perchenko, O.V. Zyuryukina, A.V. Chapurin

Abstract. **The influence of special multislit diaphragms placed in front of the receiver cathode on the signal value and signal-to-noise ratio in acoustooptical visualisation of scattering biological media is studied. Using such diaphragms the visualisation of a bulk light-absorbing and sound-transmitting object in the form of a rectangular parallelepiped with the size 5×5 mm in the plane, perpendicular to the laser beam axis, and with the size 2.5 parallel to this axis is carried out. The object was merged into scattering media of thickness $L_c = 62$ mm along the direction of propagation of the optical radiation with the parameter μL_c varying from 0 to 46 (μ being the extinction coefficient of the medium).**

Keywords: *laser radiation, ultrasound, multislit diaphragm, scattering biological medium, light-absorbing inhomogeneity, acoustooptical visualisation of inhomogeneity.*

1. Introduction

Acoustooptical tomography (AOT) is a relatively new method of visualisation of objects, hidden in strongly scattering media (to which biological media also belong). This method combines high optical contrast and spatial resolution of ultrasonic (US) tomographic systems [1–4]. The method is based on the analysis of characteristics of optical radiation passed through the scattering medium, crossed by an US beam. In this case in the alternating current of the photodetector, collecting the optical radiation, a component with the US frequency appears that carries information about the medium properties and, therefore, about the presence or absence of inhomogeneities. The AOT advantages consist in relatively low cost, absence of ionising radiation, and noninvasive nature, which is of particular interest for biotissue diagnostics in vivo. A serious obstacle for using AOT in diagnostics of light-absorbing and ultrasound-invisible inhomogeneities, hidden in scattering media, is the small value of both the useful signal and the signal-to-noise ratio. To overcome these difficulties different research groups have proposed various methods of signal detection, e.g., parallel detection using CCD-cameras [5], Fabri–Perot interferometer [6], photorefractive crystal [7], speckle-contrast detection [8], and the use of intense acoustic pulses [9].

A.P. Solov'ev, M.I. Perchenko, O.V. Zyuryukina, A.V. Chapurin
N.G. Chernyshevsky Saratov State University (National Research University), ul. Astrakhanskaya 83, 410012 Saratov, Russia;
e-mail: solovievap@yandex.ru

Received11 April 2012
Kvantovaya Elektronika **42** (5) 405–408 (2012)
Translated by V.L. Derbov

In paper [10] for wide laser beams the possibility was predicted to increase the photocurrent amplitude, corresponding to the ballistic light component, at the US frequency by installing a multislit diaphragm directly before the photocathode. For the distance between the photodetector and the US beam axis, optimal for registering the ballistic component of the current, the diaphragm should have the form of a plane grating with several similar parallel rectangular slits. The planes of the diaphragm and photocathode are perpendicular to the laser beam axis, the centre of the grating is at the axis of the laser beam, the separation between the slit centres is equal to the wavelength Λ of sound in the medium, the width of each slit is equal to 0.5Λ, and the slits are perpendicular to the direction of the sound propagation in the medium. Note, that the signal-to-noise ratio reaches its maximum at the slit width 0.375Λ.

In the present paper we experimentally study the influence of diaphragms having different number of slits on the photocurrent amplitude at the US frequency, on the sensitivity of receiving system and on the contrast and sharpness of the image in visualisation of a light-absorbing object in a scattering medium.

2. Experiment

2.1. Experimental setup

The scheme of the setup used for measurements is shown in Fig. 1. The radiation from the laser (*3*) (He–Ne laser, TEM_{00} mode, wavelength 632.8 nm, beam diameter 1.2 mm, power 6 mW) was incident on the biotissue-simulating phantom (*4*), comprising aqueous milk solution, filling the cuvette (*5*). The cuvette had the shape of a rectangular parallelepiped with the size $L_c = 62$ mm along the axis of laser radiation propagation. It was possible to place a small object, simulating a tumour, into the solution. The US transducer with the focusing lens (*2*) (the transducer diameter, 23 mm; the acoustic wavelength, $\Lambda = 0.5$ mm; the focal length, 45 mm; the focal spot diameter in water, 1.4 mm), submerged in the solution, excited a wave at the frequency 3 MHz, running normally with respect to the laser beam axis. The sound absorber (*6*) was placed in front of the transducer. Since we used the transmission scheme, the photodetector (*7*) (FEU-79) was placed in front of the laser. The signal from the photodetector was recorded using the selective voltmeter (*8*) (B6-10). The voltmeter measured alternating components of the photocurrent and noise within the bandwidth 1 kHz centred at the frequency of the US wave. If necessary, the signal from the photodetector was recorded by means of a digital oscilloscope (*9*) (DS03062A, 60 MHz, 10^9 readings per second), connected to the output of the voltme-

ter. In this case the option of averaging the measured quantity over 256 scans of oscilloscope was used, which considerably improved the accuracy of the signal measurement. As the diaphragm (*10*) we used a grating of *m* similar rectangular parallel slits with the pitch 0.5 mm, equal to the US wavelength, placed directly at the photocathode. The dimensions of each slit (width ~0.2 mm, height ~1 mm) corresponded to the maximal signal-to-noise ratio for receiving the ballistic component of the signal S_b [10]. In front of the grating the additional screen (*11*) was installed that allowed opening any single slit, three slits, or five slits. The photodetector together with the diaphragm (*10*) and the screen (*11*) could be moved along the axes *x*, *y*, and *z*. The field aperture (*12*) had the dimensions 7×8 mm along the axes *y* and *z*, respectively, and its centre was located at the axis of the laser beam.

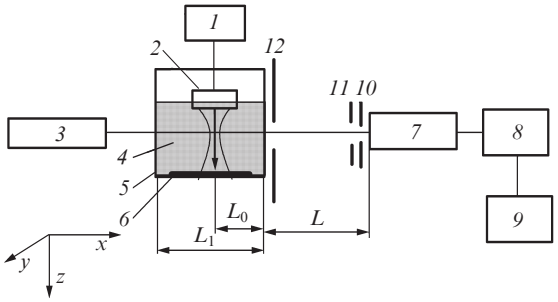

Figure 1. Schematic diagram of the experimental setup: (*1*) US generator; (*2*) US transducer; (*3*) laser; (*4*) phantom; (*5*) cuvette; (*6*) sound absorber; (*7*) photodetector; (*8*) voltmeter; (*9*) oscilloscope; (*10*) diaphragm; (*11*) auxiliary screen; (*12*) field aperture.

2.2. The technique of measurements

The selective voltmeter measured root-mean-square values of the photocurrent, hence, the useful signal *S* was calculated using the formula $S = (U^2 - N^2)^{1/2}$, where *U* and *N* are the values of photocurrent with the ultrasound generator switched on and off, respectively. In the experiment the photocurrent amplitudes at the US frequency were measured at two positions *z* of the photodetector, namely, at the axis of the laser beam (position $z_0 = 0$; U_0 and the noise N_0 measured) and beyond the geometrical dimensions of the laser beam (position $z_0 \neq 0$; U_w and N_w measured). The signal S_0 comprised the ballistic (S_b) and 'scattered' components of photocurrent, corresponding to ballistic light, passed through the medium without scattering, and the forward-scattered light. The signal S_w contained practically only the 'scattered' component. By the photomultiplier position we mean the position of the centre of the middle slit of the diaphragm (*10*).

It is convenient to compare the scattering media using the parameter μL_c (μ being the extinction coefficient of the medium), which is determined both by the properties and the thickness of the visualised medium. In the experiment the parameter μL_c was determined by the concentration *C* of the milk, which varied from 0 to nearly 2%. According to [11], at such concentrations of milk the scattering coefficient $\mu_s$value is proportional to *C* and is significantly greater than the absorption coefficient μ_a. Therefore, under the conditions of the experiment the value of μL_c was approximately equal to $\mu_s L_c$ and proportional to *C*. The proportionality coefficient was determined from the damping of the ballistic component of the signal at small concentrations *C*, when $S_b \gg S_w$. The value of μL_c varied from 0 to 46. In the process of investigations the measured quantities changed by more than 10 orders of magnitude; therefore, to provide a linear regime of photodetector operation at small μL_c we placed neutral calibrated light filters on the way of the laser beam between the cuvette with a scattering liquid and the laser (not shown in Fig. 1).

For acoustooptical imaging of a light-absorbing sound-transmitting bulk object we used grating with different number of slits. The object was a rectangular parallelepiped with the size 5×5 mm in the plane, perpendicular to the axis of the laser beam, and with the size 2.5 mm along this axis. The object was mechanically scanned with respect to the crossing point of the acoustical and optical exes in the cuvette along the coordinate axis *z* (the axis of sound propagation) and *y* axis, perpendicular to the plane (*x*, *z*), in which the axes of the laser beam (*x* axis) and the US beam (*z* axis) lie.

2.3. Experimental results and discussion

In scattering media with different values of μL_c we studied the influence of the number of diaphragm slits on the ballistic and 'scattered' components of the signal and the signal-to-noise ratio. Below the numerical subscripts in the notation of the signals mean the number of slits in the diaphragm.

Figure 2 presents the dependences of the ratio S_{0m}/S_{wm} on the parameter μL_c. It is seen that for all gratings this ratio decreases with the growth of μL_c, and starting from $\mu L_c \approx 23$ oscillates slightly beyond unity. The growth of dispersion of points with respect to the mean value, observed in Fig. 2, is related to the reduction of the measurement accuracy at small values of the measured signals.

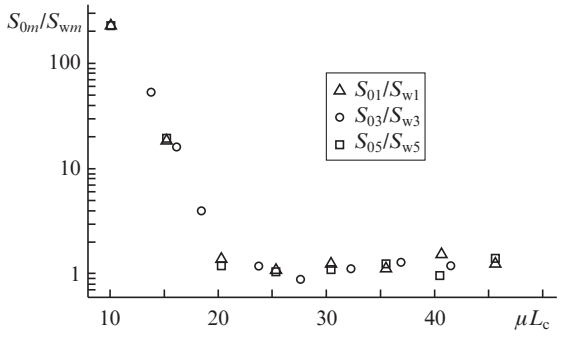

Figure 2. Dependences of the signal ratio S_{0m}/S_{wm} on the medium parameter μL_c measured using multislit diaphragms (*m* is the number of slits in the diaphragm).

Figures 3 and 4 show how the different number *m* of slits in the receiving system affects the values of signals S_{0m} and the sensitivity of the receiving system η_{0m} ($\eta_{0m} = S_{0m}/N_{0m}$). It can be seen that in the entire range of μL_c variation (from 0 to 46) increasing the number of slits in the diaphragm leads to the increase in all measured quantities. In this case the sensitivity of the receiving system grows or, at least, remains constant.

It is convenient to analyse the obtained results conditionally dividing the studied range of variation of the medium parameter μL_c into two sub-ranges. The first sub-range corresponds to the variation of μL_c from 0 to 18, where, as follows from Fig. 2, $S_{0m} \gg S_w$, i. e., the ballistic component of

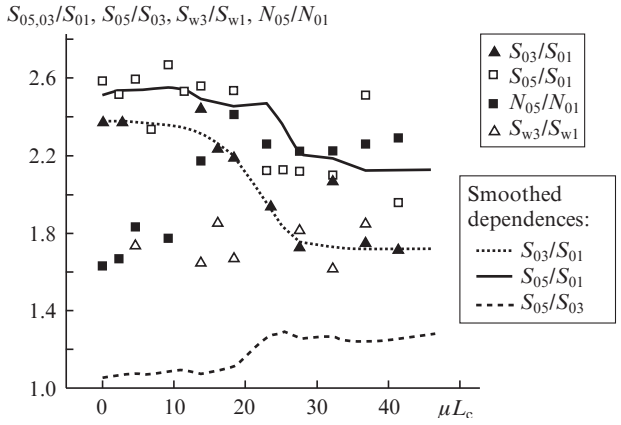

Figure 3. Dependences of the ratios of signals S_{0m}/S_{01} and S_{w3}/S_{w1} and noises N_{05}/N_{01} on the medium parameter μL_c.

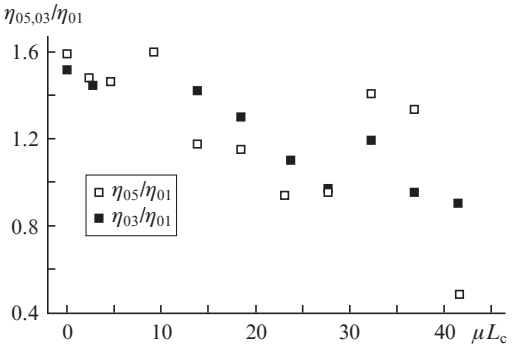

Figure 4. Dependences of the relative sensitivity $\eta = (S/N)$ of the receiving system on the medium parameter μL_c when using a three-slit (η_{03}/η_{01}) and a five-slit (η_{05}/η_{01}) diaphragm.

light causes the major contribution to the signal. In this case at constant intensity in the transverse cross section of the laser beam and the transverse beam size, exceeding the corresponding dimension of the multislit diaphragm, the ratio of signals S_{0m}/S_{01} should be equal to the number of slits m of the multislit diaphragm, because the currents from all slits at the photocathode are added in phase. The noise ratio N_{0m}/N_{01} and, therefore, the sensitivity ratio η_{0m}/η_{01} should be equal to $\sqrt{m}$. In the experiment the distribution of intensity in the laser radiation (TEM_{00} mode) is Gaussian, and the diameter of laser beam is comparable with the typical multislit diaphragm. Therefore, the intensity of the laser radiation in the area of the central slit of a multislit diaphragm will be greater than in the side slits and, therefore, the signal ratio S_{0m}/S_{01} should be smaller than m, and the noise ratio (N_{0m}/N_{01}) and the sensitivity ratio (η_{0m}/η_{01}) will be smaller than $\sqrt{m}$. In this case the sensitivity ratios exceed unity. Moreover, the aperture of the laser beam having the diameter $a_{las} \approx 1.2$ mm fits with three periods of the grating, i.e., the three-slit diaphragm having the total size $(2\Lambda + d) = 1.2$ mm. When using the grating with greater number of slits the contribution to the signal S_{0m} from the rest slits (in our case, from two side slits of a five-slit diaphragm) is expected to be insignificant. Therefore, the ratios S_{05}/S_{01} and η_{05}/η_{01} is expected to be slightly higher than the corresponding ratios S_{03}/S_{01} and η_{03}/η_{01} and the ratio S_{05}/S_{03} must be a little greater than unity. All these conclusions are in good agreement with the experimental data.

In the second sub-range ($\mu L_c > 23$) the ballistic component of the signal S_b becomes smaller than the 'scattered' component of the signal S_w, and the difference between them grows with increasing μL_c. The signals S_{0m} tend to purely scattered components S_{wm}. The same relates to the noises, i.e., $N_{0m} \approx N_{wm}$. Therefore, signal-to-noise ratios, measured at the axis of the laser beam, S_{03}/S_{01}, S_{05}/S_{01}, S_{05}/S_{03}, and N_{0m}/N_{01} are expected to be nearly equal to the ratios of signals and noises for S_{wm} and N_{wm}. In [12] it is shown that in the case of a single-slit diaphragm the 'scattered' component of the signal S_{w1} behaves similar to the noise N_{w1} with the variation of the slit width, i.e., it is also proportional to the square root of the slit area. For a diaphragm having m slits the noise N_{wm} should be proportional to $\sqrt{m}$. The results of the experiments, performed in the present study, show that the 'scattered' component of the signal S_{wm} (in Fig. 3 the dependence of S_{w3}/S_{w1} on the parameter μL_c for three slits is presented) increases with increasing number of slits by nearly $\sqrt{m}$ times in the entire range of μL_c variation, including the first range. This is an evidence of the absence of spatial correlation along the axis of sound propagation of both the scattered signal S_{wm} and the equal signal on the laser axis S_{0m} (in contrast to the ballistic signal). Hence, in the second range of μL_c variation the ratios S_{0m}/S_{01} and N_{0m}/N_{01} must be also equal to $\sqrt{m}$ and, therefore, the sensitivity ratios η_{0m}/η_{01} – approximately equal unity. These conclusions are in good agreement with the obtained experimental results: $S_{03}/S_{01} \approx 1.7 \approx \sqrt{3}$, $S_{05}/S_{01} \approx 2.2 \approx \sqrt{5}$, $S_{05}/S_{03} \approx 1.3 \approx \sqrt{5/3}$, $N_{05}/N_{01} \approx 2.4 \approx \sqrt{5}$. The sensitivity ratios η_{03}/η_{01} and η_{05}/η_{01} in the mentioned range of μL_c variation are also nearly equal to one.

Visualisation of an object, made of black polyvinyl and strongly absorbing optical radiation, was performed using gratings with different number of slits at different values of the medium parameter μL_c. Figure 5 presents the results for μL_c equal to 22 and 32. The interpretation of the results is confirmed by the dependences of the signals S_{0mn}, normalised to their mean maximal values $S_{0m\max}$, obtained with the object completely removed from the probed area. The images of the object in Fig. 5a are obtained using the measured signals S_{01n}, S_{03n}, and S_{05n} with scanning along the y axis and $z_{obj} = 0$, and in Fig. 5b with scanning along the z axis and $y_{obj} = 0$, 2.5, and 6 mm. Here z_{obj} and y_{obj} correspond to the position of the object centre with respect to the centre of the probed area, i.e., the crossing point of the laser and acoustic beam axes.

From the presented figures one can draw a conclusion that for the studied media the number of slits in the diaphragm practically does not affect the quality (contrast and sharpness) of the object image. The contrast and sharpness are practically independent of the parameter μL_c in the range 22–32. The contrast of the image, calculated using the formula $\text{contr} = (S_{\max} - S_{\min})/(S_{\max} + S_{\min})$, equals nearly 0.7 for both single-slit and multislit diaphragms. Here $S_{\min}$ is the mean value of the signal in the case of approximate coincidence of the object centre with that of the probed area. The image sharpness, which is defined as an inverse of the object displacement, corresponding to the visualisation parameter difference $(S_{\max} - S_{\min})$ changing from 0.1 to 0.9, equals nearly 0.4 mm^{-1} in both coordinates. The possibility of tomography in the scattering medium is demonstrated by three dependences of the signal S_{05n} in Fig. 5b at $\mu L_c = 22$, namely, when the centre of the moving object passes the centre of the probed area ($y_{obj} = 0$), when the edge of the object passes the centre of the probed area ($y_{obj} = 2.5$ mm), and when the whole object passes beyond the probed area ($y_{obj} = 6$ mm). Slight differ-

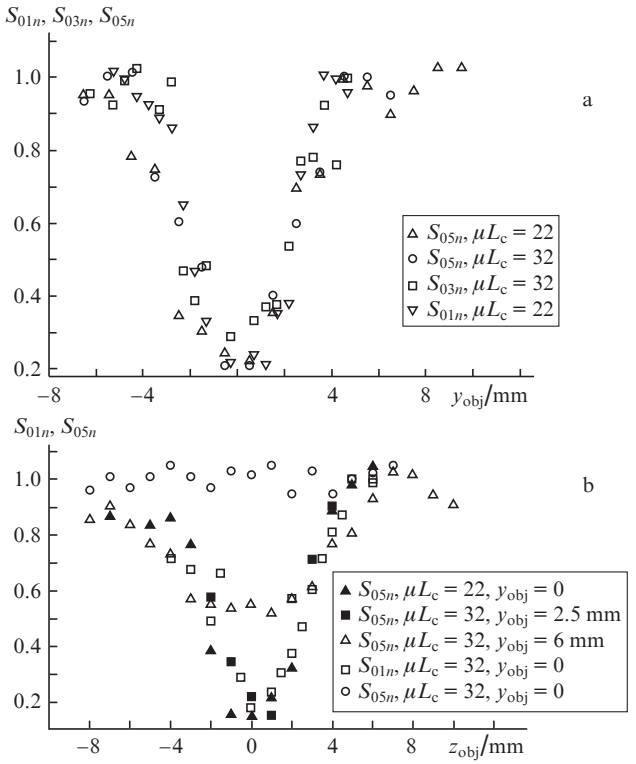

Figure 5. Dependences of the normalised signals S_{01n}, S_{03n}, and S_{05n} on the displacement of the object along the y axis at $z_{obj} = 0$, $\mu L_c = 22$ and 32 (a) and along the z axis at $y_{obj} = 0$, 2.5, and 6 mm, $\mu L_c = 22$ and 32 (b).

ence in signal values for $y_{obj} = 0$ and 2.5 mm at the object positions $z_{obj} < -6$ mm (the object is displaced towards the US source with respect to the laser beam axis) and $z_{obj} > 6$ mm is due to small absorption of the US by the object. The numerical values of the contrast and sharpness of images at $\mu L_c = 22$ coincide with similar results for a single-slit diaphragm [13, 14], where the visualisation of similar objects is considered at μL_c from 0 to 27. The results, presented in [13, 14] and in the present paper also allow selection of two ranges of μL_c values with nearly constant contrast and sharpness of images: at $\mu L_c < 18$ the contrast and sharpness are equal to 1 and 2.2 mm^{-1}, at $\mu L_c > 22$ they amount to 0.6 and 2.5 mm^{-1}, respectively. In the intermediate range of μL_c (from 18 to 22) the image contrast and sharpness quickly vary from the values at $\mu L_c < 18$ to those at $\mu L_c > 22$. The presented numerical values are approximately similar for images in both coordinates y and z.

These results may be explained as follows. The size of the probed area determines the image sharpness and contrast. At small μL_c (smaller than 18) the dimensions of the probed area are determined by the overlap of the laser and acoustic beams. In this case the size of the probed area along the directions y and z is smaller than the diameters of both the laser and the acoustic beam, which under the conditions of the experiment were approximately equal. Therefore, the contrast of a 5 × 5-mm object was equal to unity, because the object completely overlapped the probed area, while the sharpness amounted to 2.2 mm^{-1}, which corresponds to the resolution of nearly 0.5 mm, smaller than the diameters of the laser and acoustic beams. At $\mu L_c > 22$ the ballistic component of the laser radiation in the acoustic beam volume is small compared to the 'scattered' one. In this case the dimensions of the probed area are determined only by the acoustic beam (assumed that the density of the scattered laser radiation within the acoustic beam is constant). As shown in [12], for a focused acoustic beam the probed area is concentrated in the focus region, its dimensions in the y and z directions being greater than the focal spot diameter. In fact, the size of the probed area is determined by the rate of the intensity decrease in the diffraction waves with the growth of the distance from the focal plane of the acoustic beam.

3. Conclusions

We have experimentally shown that the amplitude of the signal S at the US frequency, which in the used scheme is an imaging parameter, may be increased by equipping the receiver with especially calculated diaphragms. In the range of μL_c values from 0 to 18, when the ballistic component of light introduces considerable contribution into the signal, the use of three-slit and five-slit diaphragms leads to the increase in the signal S_{03} by 2.3–2.4 times and S_{05} by 2.5–2.6 times as compared to the signal S_{01} in the case of a single-slit diaphragm. Since the size of the laser beam at the photodetector was smaller than the length of the five-slit grid along the z axis, the signal S_{05} only slightly exceeded the signal S_{03}. In this range of μL_c noticeable advantage in the sensitivity of the receiving system due to the use of multislit diaphragms was observed, $\eta_{03}/\eta_{01} \approx 1.49$, $\eta_{05}/\eta_{01} \approx 1.55$.

At $\mu L_c > 23$ the ballistic component of light is essentially smaller than the 'scattered' one, which mainly determines the signal in this case. In this range $S_{05}/S_{01} = \sqrt{5}$ and $S_{03}/S_{01} = \sqrt{3}$, which is an evidence of the absence of spatial correlation in the scattered signal. No advantage in sensitivity due to the use of multislit diaphragms was observed in this range of μL_c variation.

The visualisation of the object with characteristic size 5 × 5 mm, absorbing optical radiation and practically transparent for the acoustic signal, has shown that within the limits of high enough values of the parameter $22 < \mu L_c < 32$ the image contrast and sharpness are practically independent of the number of slits in the diaphragm and remain constant. Their values in the directions y and z are nearly similar.

References

1. Leutz M., Maret G. *Phys. B: Phys. Condensed Matter*, **204**, 14 (1995).
2. Wang L.V. *Photochem. Photobiol.*, **67**, 41(1998).
3. Kempe M., Larionov M., et al. *J. Opt. Soc. Am.*, **14** (5), 1151 (1997).
4. Tuchin V.V. *Usp. Fiz. Nauk*, **167** (5), 517 (1997) [*Phys. Uspekhi*, **40**, 495 (1997)].
5. Gross M., Goy P., Koussa M.Al. *Opt. Lett.*, **28**, 2482 (2003).
6. Sahadzie S., Wang L.H. *Opt. Lett.*, **29**, 2770 (2004).
7. Murray T.W., Sue L., Magiluri G., Roy R.A., Nieva A., Blonigen E., DiMarzio C.A. *Opt. Lett.*, **29**, 2509 (2004).
8. Li J., Ku G., Wang L.V. *Opt. Lett.*, **41**, 6030 (2002).
9. Kim C., Zemp K.I., Wang L.V. *Opt. Lett.*, **31**, 16 (2006).
10. Solov'ev A.P., Sinichkin Yu.P., et al. *Zh. Tekh. Fiz.*, **72**, 64 (2002).
11. Rinneberg H., in *Symposium and Memorian H. von Helmholtz. In The Inverse Problem* (Berlin: Akademic Verlag, 1995) p. 107.
12. Solov'ev A.P. et al. *Opt. Spektrosk.*, **100**, 245 (2006) [*Opt. Spectrosc.*, **100**, 307 (2006)].
13. Solov'ev A.P. et al. *Opt. Spektrosk.*, **92**, 345 (2002) [*Opt. Spectrosc.*, **92**, 214 (2002)].
14. Solov'ev A.P. et al. *Opt. Spektrosk.*, **101**, 305 (2006) [*Opt. Spectrosc.*, **101**, 317 (2006)].